RESEARCH PAPER

Fatigue Behavior of 4340 Steel at Room and Elevated Temperatures: Correlating Fatigue and Tensile Testing Data

Sahar Ziraki, Amir Moghaddam Kia, Ramin Ebrahimi*

* *ebrahimy@shirazu.ac.ir*

Department of Materials Science and Engineering, School of Engineering, Shiraz University, Shiraz, Iran

Received: October 2025 **Revised: October 2025** **Accepted: November 2025**
DOI: 10.22068/ijmse.4368

Abstract: *In this study, an existing approach for estimating fatigue life using tensile data was extended and applied to 4340 steel under different temperatures. The S-N and strain-life curves were plotted at 25, 200, and 350°C. The Basquin and Coffin-Manson equation constants were determined based on the corrected actual fracture stress and strain values. Moreover, the b constants were approximated as -0.065, -0.072, and -0.073 at 25, 200, and 350°C, respectively. This was achieved by setting the alternating stress equal to the fatigue limit in an infinite number of cycles when the b levelled off. The transition fatigue life of 1000 cycles was considered for 4340 steel to determine the c constants, which were found to be -0.69, -0.7, and -0.699 at 25, 200, and 350°C, respectively. The strain-life curves were then plotted. Comparison of S-N curves derived from both fatigue and tensile data showed strong agreement, indicating that the tensile test is a cost-effective, straightforward method that provides a quick estimate of high- and low-cycle fatigue behaviour and is a suitable alternative to conventional fatigue testing.*

Keywords: *S-N curve, Fatigue test, Tensile test, 4340 steel.*

1. INTRODUCTION

The failure of engineering components is a significant issue that has been the subject of extensive research for many years. Since failures of critical components in structures or vehicles can cause catastrophic damage, predicting component lifespans is crucial [1, 2]. With the advancement of industry and the increasing use of devices such as automobiles, compressors, pumps, turbines, and aircraft, which are subjected to repetitive and vibrational loading, the need to further investigate fatigue has arisen [3]. When components are subjected to cyclic loading, they may fail at stresses far below their ultimate or yield strength, a phenomenon known as fatigue, which is considered the leading cause of many mechanical failures in industry [4–7]. Therefore, investigating the fatigue behaviour of metals and identifying structures with the most significant resistance to fatigue has received much attention in recent years and is a critical need for most industries [8, 9]. Therefore, it is of great importance to prevent fatigue failure, either by designing fatigue-resistant materials that can withstand dynamic loading over an infinite fatigue life or by replacing components before any failure or damage occurs. To investigate the fatigue behavior of materials, a large number of samples are required. Furthermore, fatigue tests are time-consuming and complex due to the application of cyclic loading. Therefore, identifying alternative approaches to studying the fatigue behaviour of materials is highly valuable. A wide variety of studies have been conducted to tackle this issue. For example, Strzelecki and Tomaszewski [10] explored the prediction of fatigue S-N curve using hardness measurements. Roessle and Fatemi [11] investigated the use of hardness data and modulus of elasticity (E) to estimate fatigue behavior. Tensile test data have long been used to evaluate fatigue properties. In several studies, tensile data, such as ultimate tensile strength (UTS), yield strength (YS), and reduction in area (RA), have been used or developed to predict fatigue properties, mostly based on empirical correlations between tensile and fatigue properties [12]. For instance, Manson [13] proposed the universal slopes method and four-point correlation method in 1965, which were later revised by him and his colleagues [14]. Yang et al. [15] reviewed and summarised various models used to predict fatigue life under low-cycle loading conditions. Therefore, various methods can be employed to investigate the fatigue behavior, each with its own advantages and limitations. Some of these methods are valid only for specific groups of materials, while for others, such as Al alloys, they show significant errors. To select the best and most appropriate method among these methods, Park et al. [16] proposed an expert system that can

[DOI: 10.22068/ijmse.4368]

be effectively utilised for practical applications.
In this study, we intend to propose a cost-effective and straightforward method for predicting fatigue behavior more efficiently using the tensile test. The tensile test is one of the most fundamental and widely used methods for investigating the mechanical properties of materials. It is a straight-forward technique that requires less testing time. This study aims to determine the constant parameters of the Basquin equation, which describes the fatigue behaviour of materials. Therefore, by conducting only a single tensile test, the fatigue S-N curve can be obtained. The idea of estimating fatigue behaviour solely from simple tensile test results was first introduced by Ebrahimi et al. [17]. Nevertheless, since they did not perform their own fatigue experiments to validate the proposed method, the use of previously published fatigue data provided only weak support for their approach. In this study, to investigate fatigue behaviour and compare the results with those from tensile testing, tests were performed on 4340 steel due to its high potential. AISI 4340 steel is among a group of steels known as high-strength low-alloy steels (HSLA) [18, 19]. It is a medium carbon steel containing less than 8% alloying elements, exhibiting a combination of properties such as high strength, hardenability, good toughness, high fatigue strength, and good crack resistance [20]. These properties make it a widely used material to manufacture structural components that demand both high strength and toughness, particularly in the aerospace and automotive industries [21–23].

2. EXPERIMENTAL PROCEDURES

2.1. Heat Treatment Procedure

In this study, AISI 4340 steel was used, with the chemical composition shown in Table 1. This steel is prone to the formation of undesirable inclusions and carbides due to the presence of certain alloying elements. To prevent the formation of such inclusions, the as-received steel was cast under vacuum conditions.
4340 steel is a heat-treatable alloy whose strength and properties are strongly dependent on the heat treatment applied [24]. To obtain an appropriate microstructure with high strength and toughness simultaneously, a two-step heat treatment of quenching and tempering was performed on this steel, as shown in Fig. 1. According to this diagram, at the first stage of the process, the steel was preheated at 600°C for 1 h, followed by austenitizing at 850°C for 50 min. Next, it was quenched in oil at 65°C. Since martensitic structures are very brittle, tempering was performed to increase the steel's fracture toughness. To serve this purpose, the steel was placed in a furnace, and its temperature was gradually increased to 480°C. The steel was held in the furnace at this temperature for 3 h, allowing for annealing and the transformation of martensite into tempered martensite. Then, the steel was slowly cooled to ambient temperature. Reaching ambient temperature, the steel underwent a secondary annealing process. It was held at 480□ for an additional 90 min to allow new grains to nucleate and grow. Finally, the sample was slowly cooled to the ambient temperature.A scanning electron microscope (SEM; Leica Cambridge) was used to examine the sample's microstructure.

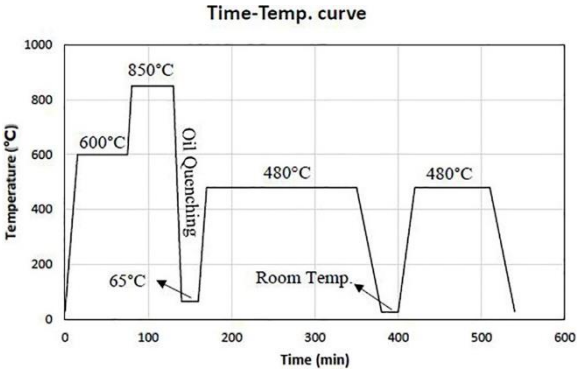

Fig. 1. Heat treatment process of 4340 steel

2.2. Tensile Test

The tensile tests were carried out at 25, 200, and 350°C with a crosshead speed of 5 mm/min, using the Santam (STM-600) universal testing machine. Fig. 2 shows the dimensions of the dogbone tensile specimen. This test was repeated three times to ensure the reliability of the results.

2.3. Rotating Bending Fatigue Test

In this study, a rotating bending fatigue test was used to investigate the fatigue behavior of 4340 steel at 25, 200, and 350°C.

Table 1. Chemical composition of 4340 alloy

Elements	Fe	C	Ni	Cr	Mo	Mn	Si	S	P
wt.%	93.4	0.32	3.18	1.42	0.41	0.59	0.31	0.008	0.02

[DOI: 10.22068/ijmse.4368]

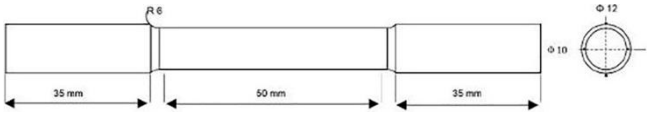

Fig. 2. Dogbone tensile test specimen dimensions

The test was performed at a rotational speed of 3000 rpm (50 Hz) using a MARUI & CO., LTD. device from Japan. To investigate fatigue behaviour at high temperatures, a custom-designed 220 V electric furnace was built. Two thermocouples were used to precisely control the temperatures of both the furnace and the specimen surfaces. The test specimens were designed as cantilever beams according to ASTM E466, and their surfaces were entirely polished to minimize the sources of errors, Fig. 3. The test began at a stress level corresponding to 70% of the yield stress, and the subsequent specimens were gradually subjected to lower stress levels to obtain the S-N curve. The applied stress was calculated using Eq. (1):

$$\sigma = {}^{MC}/_{I} \quad (1)$$

Where M is the bending moment (F × L), C is the radius of the specimen, and I is the moment of inertia.

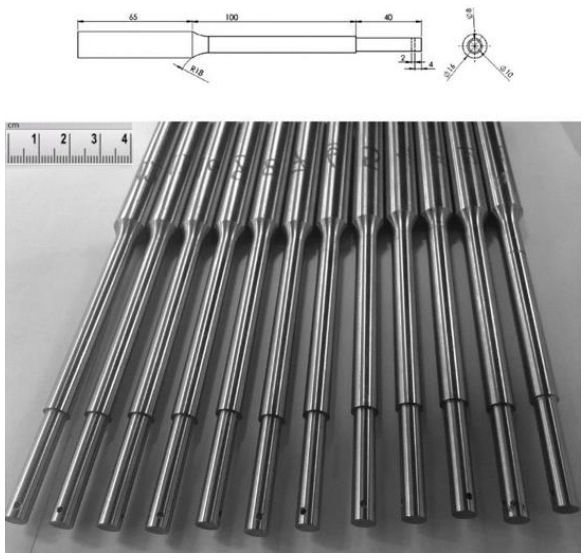

Fig. 3. Geometry and dimensions of the fatigue test specimens in accordance with ASTM E466

Some equations can approximate the S-N curve, and one of the best relationships used to mathematically describe the fatigue life behavior in terms of stress is the Basquin relationship [25]:

$$\sigma_a = \sigma_f'(2N_f)^b \quad (2)$$

Where σ_a is the alternating stress or stress amplitude under completely reversed loading ($\sigma_m = 0$), N_f is the number of cycles to failure, and σ_f' and b are materials properties. If the parameters σ_f' and b are known, the Basquin equation can be approximated, enabling the prediction of fatigue behaviour. Therefore, our novel approach in this study is to determine these parameters to obtain the Basquin equation.

To estimate the physical infinity, the constant b is suggested to be calculated for different cycle numbers by considering $\sigma_a = \sigma_e$, where σ_e is the fatigue limit below which the lifetime is infinite. It is approximated to be $0.5\sigma_{UTS}$ for materials such as steels with $\sigma_{UTS} < 1400$ MPa [26].

σ_f' is often approximately the same as the actual stress at the fracture point obtained from the tensile test, because the tensile test can be regarded as half-cycle fatigue life (N_f= 0.5) when failure occurs [27]. As a result, a simple tensile test can be performed to obtain S-N and Coffin-Manson curves, which is less time-consuming and requires only one sample. However, the fatigue results from the tensile test must first be validated. Hence, this study intends to examine the consistency of results obtained from both tensile and fatigue testing to assess the precision and reliability of using tensile test data for fatigue life prediction in 4340 steel.

3. RESULTS AND DISCUSSION

Fig. 4 depicts the SEM image of the 4340 steel microstructure after two-stage heat treatment. This structure mainly consists of ferrite and precipitated carbides (white color), as well as bainite. This indicates that oil-quenching steel results in a mixed bainitic and martensitic structure. By tempering the steel at 480°C, the martensite phase decomposes into ferrite and carbide precipitates. This structure contributes to high strength and toughness simultaneously. The mechanical properties of 4340 steel were investigated using a tensile test, as described below. As tensile data are used to determine the fatigue behavior of 4340 steel, it is necessary to accurately estimate the true stress-strain diagrams. Therefore, to correct the necking effect in the tension specimens, i.e., the triaxial stress state in the necking region, the Bridgman correction factor [28] was applied as Eq. (3):

[DOI: 10.22068/ijmse.4368]

$$\sigma_B = \sigma\left[\left(1+\frac{2R}{a}\right)\ln\left(1+\frac{a}{2R}\right)\right]^{-1} \quad (3)$$

Where σ_B is the corrected value of stress, σ is the calculated actual stress, $\sigma = F/A$ (where F and A denote the applied force and the actual cross-sectional area, respectively), a is the radius of the necking region, and R is the radius of neck curvature.

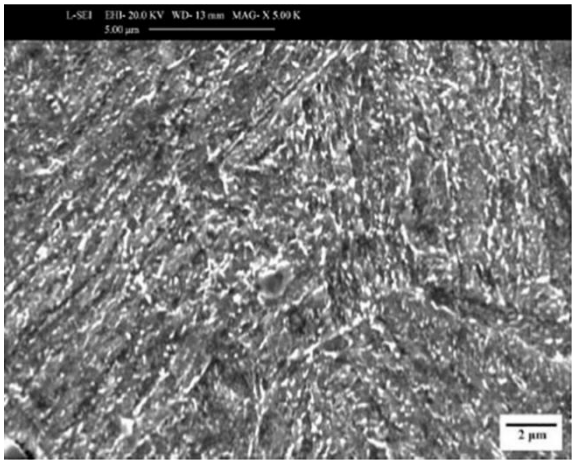

Fig. 4. SEM image of the microstructure of 4340 steel after two-stage heat treatment (Etched with 2% Nital solution)

To measure the neck curvature radius at the end of the tensile test, the fractured parts were assembled and photographed at the point of failure. Fig. 5 shows the tensile specimen after testing at 25°C, used to determine the radii R and a. Based on Eq. (3), the Bridgman correction factors were calculated as 0.84, 0.81, and 0.83 at 25, 200, and 350°C, respectively. The true strain and stress at the fracture point were calculated using $\varepsilon = \ln A_\circ/A = 2\ln D_\circ/D$ and $\sigma = F_f/A_f$ and the true stresses obtained at 25, 200, and 350°C, respectively, were 1711, 1808, and 1742 MPa. The corrected true stresses, using Bridgman correction factors, were obtained to be 1442, 1475, and 1453 MPa at 25, 200, and 350°C, respectively.

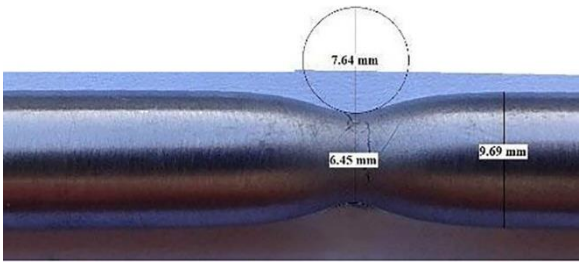

Fig. 5. Typical tensile test specimen after fracture, used to measure the minimum diameter and radius of curvature in the necking region

Another method for plotting the actual stress-strain curve after necking is based on the power-law approximation. This equation, which describes the relationship between actual stress and true strain in the uniform plastic deformation region, is given by:

$$\sigma = K\varepsilon^n \quad (4)$$

Where K and n are the strength coefficient and the strain hardening exponent, respectively. By taking the natural logarithm of both sides of Eq. (4), the equation becomes:

$$\ln\sigma = \ln K + n\ln\varepsilon \quad (5)$$

Using the stress-strain data in the uniform plastic deformation region, as shown in Fig. 6, the values of K and n were determined, as shown in Table 2. Normally, the strain hardening rate decreases with increasing temperature. However, at intermediate temperatures, due to dynamic strain ageing, solute atoms may diffuse and limit dislocation motion, which can lead to an increase in the strain hardening rate [29].

Table 2. The values of K and n at 25, 200, and 350°C

	25°C	200°C	350°C
K (MPa)	1500	1442	1434
n	0.07	0.09	0.1

By using Eq. (4) and the calculated n and K values, the actual stress-strain curve after necking can be extended to the fracture point. This method was used to calculate true stresses and strains after necking because the equations, i.e., $\varepsilon = \ln(1+e)$ and $\sigma = S(1+e)$, that relate the true and engineering stresses and strains are no longer valid, as Al=constant cannot be assumed in this region. The engineering and corrected proper stress-strain curves obtained by these methods are depicted in Fig. 7. The true fracture stresses calculated by this method are very close to the values obtained using the Bridgman equation. Therefore, both methods can be used to determine the σ_f' to investigate fatigue behavior. The ultimate tensile strengths of 1151, 1038, and 1010 MPa were obtained from the engineering curves at 25, 200, and 350°C, respectively. As expected, σ_{UTS} decreases with increasing temperature. Therefore, the fatigue limits were estimated using $\sigma_e = 0.5\sigma_{UTS}$. Since the test temperatures ($\leq$ 350°C) are below the threshold for significant oxidation or creep, thermal softening effects were assumed minimal. To determine the constant b, as outlined in the Materials and Methods section, b was calculated for an unlimited number of cycles (e.g., at 350°C, b= $\ln(505/1453)/\ln(2N_f)$).

[DOI: 10.22068/ijmse.4368]

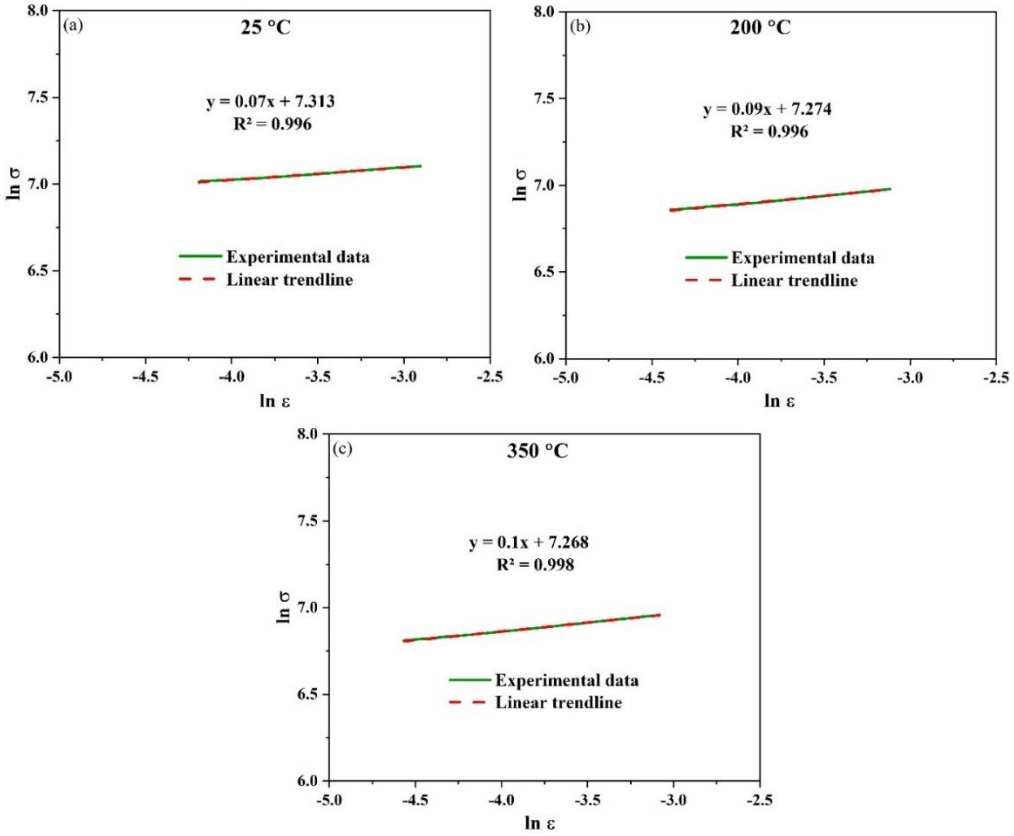

Fig. 6. Linear fitting of true stress-strain data to determine n and K at: a) 25°C, b) 200°C, and c) 350°C

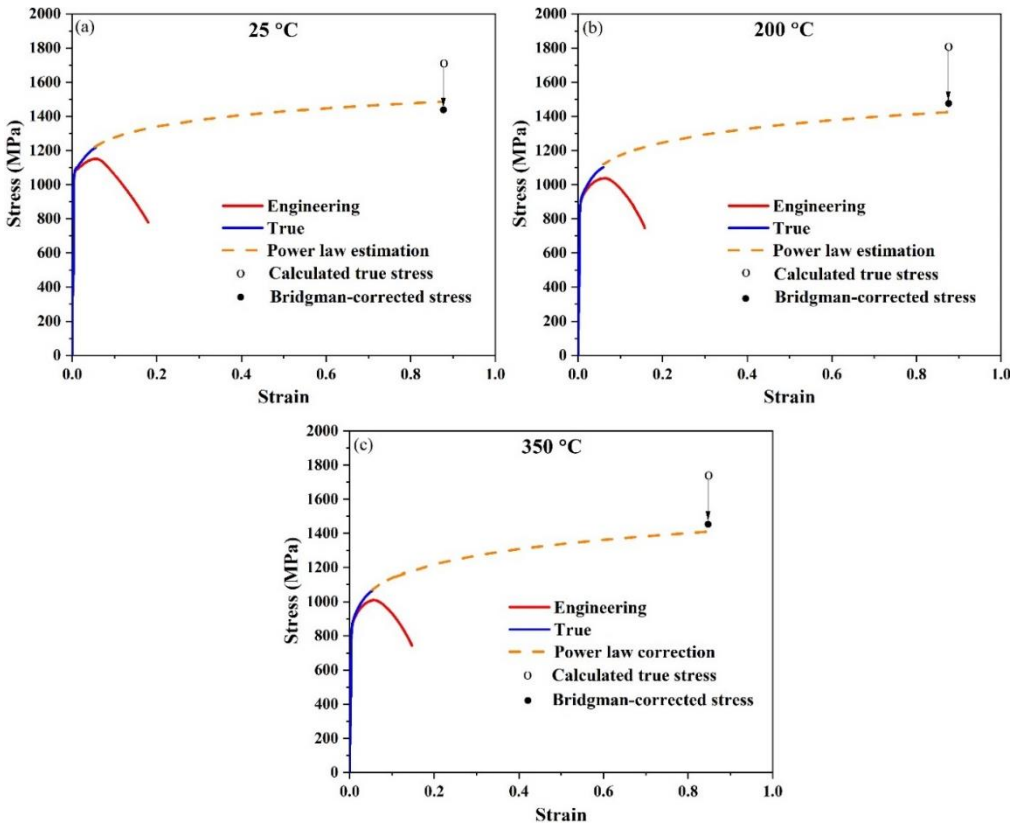

Fig. 7. True and engineering stress-strain curves of 4340 steel at a) 25°C, b) 200°C, and c) 350°C

[DOI: 10.22068/ijmse.4368]

As shown in Fig. 8, the b values increased sharply and stabilised at approximately -0.065, -0.072, and -0.073 after 10^6 cycles at 25, 200, and 350°C, respectively. Using these parameters, the Basquin equations can be determined. Similar to the method used to determine n and K in the power law equation, the Basquin constants were approximated by taking the natural logarithm of both sides of the Basquin equation as follows:

$$\ln \sigma_a = \ln \sigma'_f + b \ln 2N_f \quad (6)$$

Fig. 9(a) shows the linear fit of the fatigue test data at 25°C, where b is the slope (=-0.126) and $\ln \sigma'_f$ is the y-intercept ($\ln \sigma'_f = 7.932$, $\sigma'_f = 2785$ MPa). Similarly, the b and σ'_f values at 200 and 350°C, as shown in Figs. 9(b) and 9(c) were obtained as -0.154 and 3699 MPa, and -0.121 and 2504 MPa, respectively.

The difference between the σ'_f values calculated from the fatigue test and tensile test can be attributed to the fact that the fatigue test was performed using the rotating bending method. If the fatigue test had been carried out using the push-pull technique, σ'_f might be expected to show greater agreement between the two tests. By determining these parameters, σ_a can be calculated for different cycle numbers, and the S-N curves can be fitted on fatigue data and plotted, as shown in Fig. 10. For better comparison, the S-N curves obtained from the fatigue tests and those that can be derived from tensile data were plotted in Fig. 10. This figure shows that as the amount of stress applied to the sample increases, the number of cycles to failure decreases. After about 10^5 cycles, the dependence of fatigue life on stress is greatly reduced until it reaches the fatigue limit, which is approximately 50% of the ultimate tensile strength. At higher temperatures, materials deform more easily due to an increase in the number of active slip systems and a reduction in the stress required for dislocation movement. Therefore, with increasing temperature, the material's resistance to deformation decreases, and the fatigue crack nucleation mechanism known as intrusion-extrusion is activated at lower stress levels.

This results in a decrease in the material's fatigue strength. Besides, as the temperature increases, diffusion increases and fine carbides turn into coarser precipitates, which can reduce the fatigue strength of the material. As shown, there is good agreement between the S-N curves obtained from tensile and fatigue test data, indicating that the proposed approach of approximating fatigue behaviour from tensile test data is a reliable technique. This is a promising result, as the tensile test is a simple, accessible, and economical method.

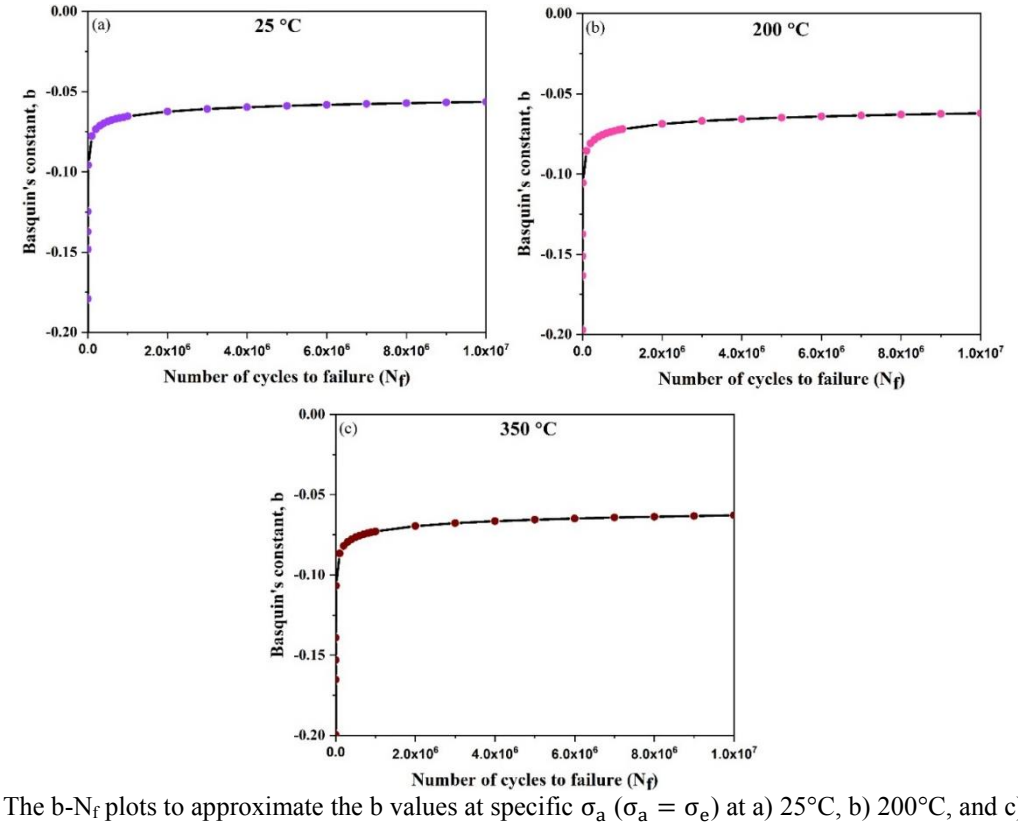

Fig. 8. The b-N_f plots to approximate the b values at specific σ_a ($\sigma_a = \sigma_e$) at a) 25°C, b) 200°C, and c) 350°C

[DOI: 10.22068/ijmse.4368]

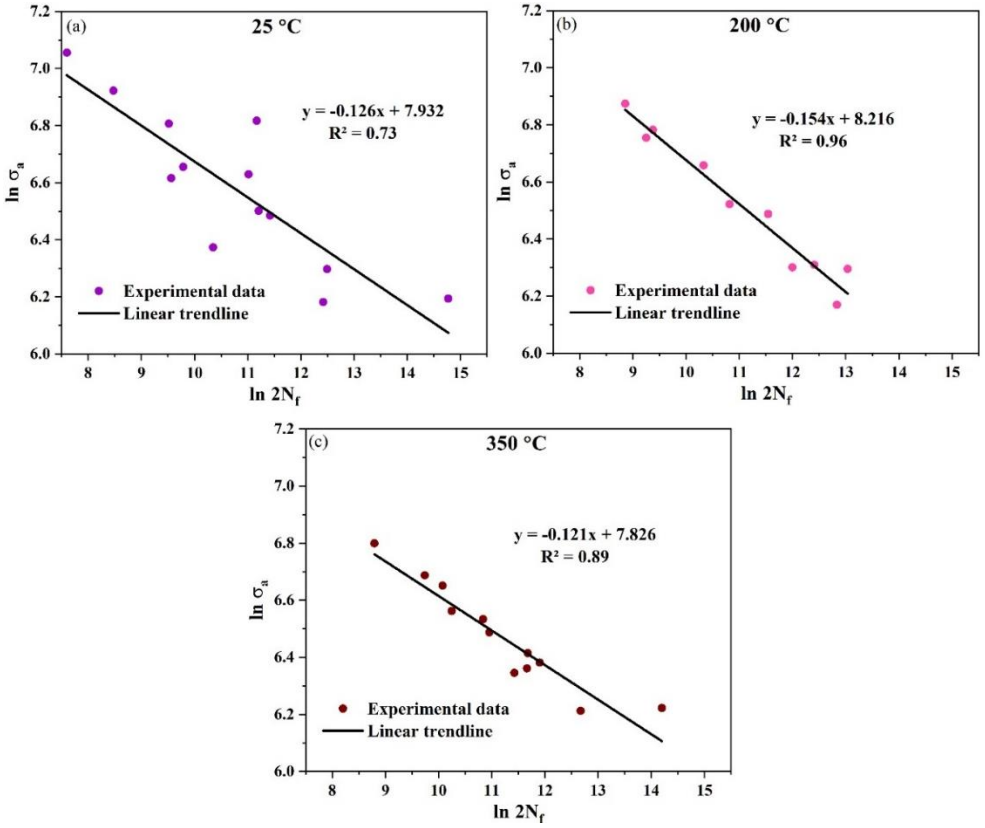

Fig. 9. The ln σ_a -ln $2N_f$ plots used to determine the Basquin constants based on the fatigue test data at a) 25°C, b) 200°C, and c) 350°C

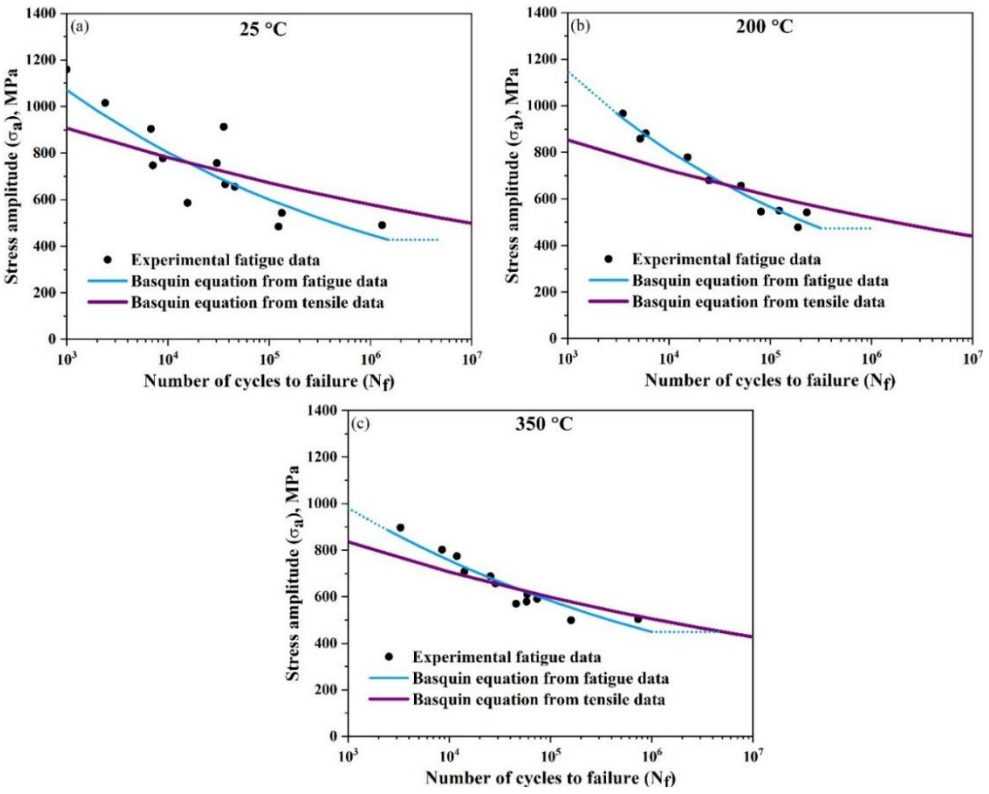

Fig. 10. The S-N curves plotted on a logarithmic scale, obtained from tensile data compared with the curves obtained from fatigue tests at a) 25°C, b) 200°C, and c) 350°C

[DOI: 10.22068/ijmse.4368]

To compare the fatigue limit and Basquin constant values obtained from the tensile data approach and from experimental fatigue data, Table 3 is presented at 25, 200, and 350°C. Moreover, the strain-based approach can also be investigated to estimate fatigue life using this novel method. In this approach, the strain-life curve is plotted instead of the S-N curve. It is mainly applied to materials with short fatigue lives or low-cycle fatigue behavior, in which plastic deformation plays a significant role. The total strain amplitude (ε_a), which includes both elastic ($\varepsilon_{ea} = \sigma_a/E$) and plastic parts ($\varepsilon_{pa}$), is given by [30]:

$$\varepsilon_a = \varepsilon_{ea} + \varepsilon_{pa} = \frac{\sigma'_f}{E}(2N_f)^b + \varepsilon'_f(2N_f)^c \quad (7)$$

This is a comprehensive approach that can be applied to both short- and long-life fatigue. This equation, known as the Coffin-Manson equation, includes the Basquin equation in its elastic part. c is the slope of the plastic part of the log-log plot, similar to the b constant in the elastic region. ε'_f is the true fracture strain calculated from the tensile test. To approximate the strain-life curve using tensile data, the constant c must be determined. The novel approach proposed here is to consider the transition fatigue life (N_t) of 1000 cycles [30]. The transition fatigue life is defined as the point where the two diagrams of elastic and plastic strain meet, i.e., when $\varepsilon_{ea} = \varepsilon_{pa}$. It means that below this crossing point, i.e., in the low-cycle fatigue region, the plastic term is dominant, while above N_t, i.e., in the high-cycle fatigue region, the elastic term becomes dominant. N_t can be determined as follows:

$$N_t = \frac{1}{2}\left(\frac{\sigma'_f}{\varepsilon'_f E}\right)^{\frac{1}{c-b}} \quad (8)$$

By considering $N_t = 1000$, the c constants can be calculated, as the other material constants are known. The resulting c values are -0.69, -0.7, and -0.699 at 25, 200, and 350°C, respectively. With these, the elastic, plastic, and total strain curves can be plotted, as shown in Fig. 11.

Table 3. The values of fatigue limit and Basquin constant obtained from the tensile data approach and the experimental fatigue data at 25, 200, and 350°C

	25 °C	200 °C	350 °C
σ_e (MPa)	575.5	519	505
b	-0.065 (from tensile data) -0.126 (from fatigue data)	-0.072 (from tensile data) -0.154 (from fatigue data)	-0.073 (from tensile data) -0.121 (from fatigue data)
σ'_f (MPa)	1486 (from tensile data) 2785 (from fatigue data)	1475 (from tensile data) 3699 (from fatigue data)	1453 (from tensile data) 2504 (from fatigue data)

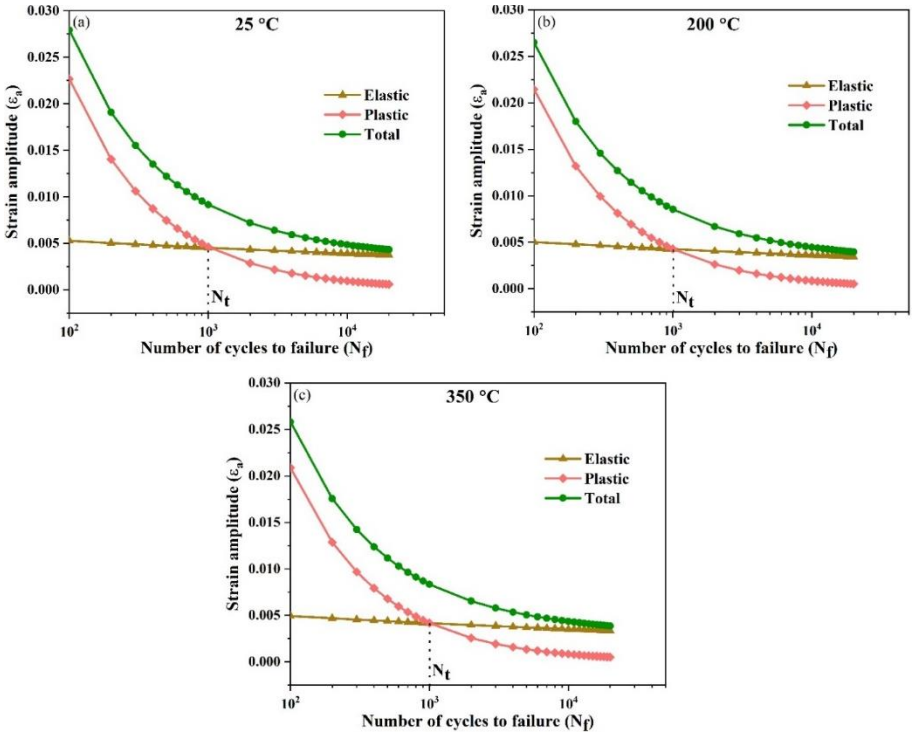

Fig. 11. Strain-life curves (logarithmic scale) approximated for 4340 steel using tensile test data at a) 25°C, b) 200°C, and c) 350°C

[DOI: 10.22068/ijmse.4368]

For the purpose of comparison, the strain-life curve obtained from this approach at 25°C and those extracted from fatigue test results in literature [24, 31] were illustrated in Fig. 12. The diagrams are closely matched, demonstrating the validity of this approach. Therefore, the method of approximating fatigue behavior using tensile test data can be applied to both stress- and strain-based approaches. By way of conclusion, while this study's results show the reliability of the proposed approach for 4340 steel, it remains to be seen how accurate this efficient method is for other metals, such as Mg and Al alloys. This certainly needs extensive future research to identify and refine the associated challenges and limitations, enabling accurate evaluation of fatigue properties.

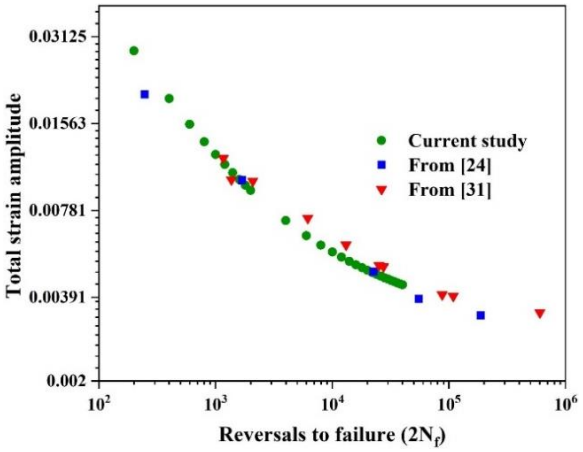

Fig. 12. Strain-life curve, on a logarithmic scale, using tensile data and comparing it with diagrams obtained from the fatigue test in the literature

4. CONCLUSIONS

In this study, the fatigue behavior of 4340 steel at 25, 200, and 350°C was estimated using tensile test data. To plot the S-N curves, the Basquin constants, i.e., b and σ_f' were calculated. The values of σ_f' were estimated from the corrected true stress at the fracture points. The constants b were obtained from the b-N curves when b reached a plateau under an infinite number of cycles, considering a fatigue limit of $0.5\sigma_{UTS}$. To estimate the strain-life curves, the Coffin-Manson equations were applied by calculating their constants, i.e., c and ε_f', where ε_f' is equal to the true fracture strain. The c constants of -0.69, -0.7, and -0.699 were calculated by considering the transition fatigue life (N_t) of 1000 cycles.

The S-N and strain-life curves obtained from these approaches were consistent with those derived from fatigue test data. The results revealed that this novel approach offers a promising, practical way to evaluate the fatigue properties of materials.

ACKNOWLEDGMENT

Financial support by the office of the Research Council of Shiraz University (Shiraz, Iran) through grant nmber 03-GR-ENG 15 is appreciated.

REFERENCES

[1] Nishida, S. I., Failure Analysis in Engineering Applications, Elsevier, Boston, USA. 2014. doi: 10.1016/C2013-0-06527-9.

[2] Wulpi, D. J., Understanding How Components Fail. ASM International, Materials Park, second ed., Ohio, USA, 2013.

[3] Callister, W. D., and Rethwisch D. G., Fundamentals of Materials Science and Engineering, John Wiley & Sons, sixth ed., Singapore, 2022.

[4] Li, B. C., C. Jiang, X. Han, and Y. Li. "A New Approach of Fatigue Life Pediction for Metallic Materials Under Multiaxial Loading". Int. J. Fatigue, 2015, 78, 1-10. doi: 10.1016/j.ijfatigue.2015.02.022.

[5] Bathias, C., and Pineau, A., Fatigue of Materials and Structures: Application to Design and Damage, John Wiley & Sons, 2013.

[6] Weiss, M. P., and Lavi, E., "Fatigue of Metals—What the Designer Needs?", Int. J. Fatigue, 2016, 84, 80–90. doi: 10.1016/j.ijfatigue.2015.11.013.

[7] Voorwald, H. J. C., Rocha, P. C. F., Cioffi, M. O. H., and Costa, M. Y. P., "Residual Stress Influence on Fatigue Lifetimes of Electroplated AISI 4340 High Strength Steel", Fatigue Fract. Eng. Mater. Struct., 2007, 30, 1084–1097. doi: 10.1111/j.1460-2695.2007.01178.x.

[8] Shiozawa, K., Murai, M., Shimatani, Y., and Yoshimoto, T., "Transition of Fatigue Failure Mode of Ni–Cr–Mo Low-Alloy Steel in Very High Cycle Regime", Int. J. Fatigue, 2010, 32, 541–550, doi: 10.1016/j.ijfatigue.2009.06.011.

[9] Yonezawa, T., Luo, P., and Tsutsumi, S., "Evaluation of Fatigue Crack Initiation and Propagation Properties of Structural Steels with Different Cyclic Softening Behavior Based on Local Strain", ISIJ Int., 2024, 64,

[DOI: 10.22068/ijmse.4368]

1477–1485, doi: 10.2355/isijinternational. ISIJINT-2024-124.
[10] Strzelecki, P., and Tomaszewski, T., "Analytical Models of the S–N Curve Based on the Hardness of the Material", Procedia Struct. Integr., 2017, 5, 832–839, doi: 10.1016/j.prostr.2017.07.065.
[11] Roessle, M. L., and Fatemi, A., "Strain-Controlled Fatigue Properties of Steels and Some Simple Approximations", Int. J. Fatigue, 2000, 22, 495–511.
[12] Özdeş H., and Tiryakioğlu, M., "On Estimating High-Cycle Fatigue Life of Cast Al-Si-Mg-(Cu) Alloys from Tensile Test Results", Mater. Sci. Eng. A, 2017, 688, 9–15, doi: 10.1016/j.msea.2017.01.106.
[13] Manson, S. S., "Fatigue: A Complex Subject—Some Simple Approximations", Exp. Mech., 1965, 5, 193–226.
[14] Muralidharan, U., and Manson, S. S., "A Modified Universal Slopes Equation for Estimation of Fatigue Characteristics of Metals", J. Eng. Mater. Technol., 1988, 110, 55–58, doi: 10.1115/1.3226010.
[15] Yang, S., Yang, L., and Wang, Y., "Determining the Fatigue Parameters in Total Strain Life Equation of a Material Based on Monotonic Tensile Mechanical Properties", Eng. Fract. Mech., 2020, 226, 106866, doi: 10.1016/j.engfracmech.2019.106866.
[16] Park, J. H., Song, J. H., Lee, T., and Lee, K. S., "Implementation of Expert System on Estimation of Fatigue Properties from Monotonic Mechanical Properties Including Hardness", Procedia Eng., 2010, 2, 1263–1272, doi: 10.1016/j.proeng.2010.03.137.
[17] Ebrahimi, R., Reihanian, M., and Namvarian. R., "A Novel Approach for Estimating Fatigue Behavior of Stainless Steel 304 Using Tensile Test Data". International Journal of Iron & Steel Society of Iran, 2024, 21, 45-50, doi: 10.22034/IJISSI. 2024.2042421.1304.
[18] Branco, B R., and Berto, F., "Mechanical Behavior of High-Strength, Low-Alloy Steels", Metals, 2018, 8, 610, doi: 10.3390/met8080610.
[19] Liu, Y., Shi, L., Liu, C., Yu, L., Yan, Z., and Li, H., "Effect of Step Quenching on Microstructures and Mechanical Properties of HSLA Steel", Mater. Sci. Eng. A, 2016, 675, 371–378, doi: 10.1016/j.msea.2016.08.087.
[20] ASM International Handbook Committee, Materials Selection and Design, S. Lampman and G.E. Dieter, ed., ASM Handbook. Mater. Sel. Des., Taylor & Francis, 1997.
[21] Çalışkan, S., and Gürbüz, R., "Determining the Endurance Limit of AISI 4340 Steels in Terms of Different Statistical Approaches", Frat. Ed Integrita Strutt., 2021, 344–364, doi: 10.3221/IGF-ESIS.58.25.
[22] Goanță, V., Munteanu, C., Müftü, S., Istrate, B., Schwartz, P., Boese, S., Ferguson, G., Morăraș, C.I., and Stefan, A., "Evaluation of the Fatigue Behavior and Failure Mechanisms of 4340 Steel Coated with WIP-C1 (Ni/CrC) by Cold Spray", Materials, 2022, 15, 8116, doi: 10.3390/ma15228116.
[23] de Souza Martins Cardoso, A., Abdalla, A. J., Reis Pereira Baptista, C. A., and de Lima, M. S. F. "Comparison of High Cycle Fatigue in 4340 and 300M Steel Welded with Fiber Laser", Adv. Mater. Res., 2014, 891–892, 1507–1512, doi: 10.4028/www.scientific.net/AMR.891-892.1507.
[24] Pape, J. A., and Neu, R. W., "A Comparative Study of the Fretting Fatigue Behavior of 4340 Steel and PH 13-8 Mo Stainless Steel", Int. J. Fatigue, 2007, 29, 2219–2229, doi: 10.1016/j.ijfatigue.2006.12.016.
[25] Meyers M. A., and Chawla, K. K., Mechanical Behavior of Materials, Cambridge University Press, second ed., New York, USA, 2009.
[26] Marghitu, D., Diaconescu, C .I., and Ciocirlan, C. I., "Mechanics of Materials, in D.B. Marghitu", Ed., Mech. Eng. Handb., Academic Press, 2001, 119–188, doi: 10.1016/B978-012471370-3/50004-8.
[27] Dowling, N. E., Mechanical Behavior of Materials: Engineering Methods for Deformation, Fracture, and Fatigue, Pearson, fourth ed., Boston, USA, 2013.
[28] Hosford W. E., and Caddell, R. M., Metal Forming Mechanics and Metallurgy, Cambridge University Press, fourth ed., New York, USA, 2011.
[29] Akbarpour, M. R. and Ekrami, A., "Effect of temperature on flow and work hardening behavior of high bainite dual phase (HBDP) steels", Mater. Sci. Eng. A., 2008, 475(1-2), 293-298. doi: 10.1016/j.msea. 2007.04.099
[30] Dieter, G. E., and Bacon, D., Mechanical

[DOI: 10.22068/ijmse.4368]

Metallurgy, second ed., McGraw-Hill, New York, USA, 1976.

[31] Tartaglia, J. M., and Hayrynen, K. L., "A Comparison of Fatigue Properties of Austempered Versus Quenched and Tempered 4340 Steel", J. Mater. Eng. Perform., 2012, 21, 1008–1024, doi: 10.1007/s11665-011-9951-y.

[DOI: 10.22068/ijmse.4368]